Eksploatacja i Niezawodnosc – Maintenance and Reliability
Volume 22 (2020), Issue 4
journal homepage: http://www.ein.org.pl

Article citation info:
Zuber N, Bajrić R. Gearbox faults feature selection and severity classification using machine learning. Eksploatacja i Niezawodnosc – Maintenance and Reliability 2020; 22 (4): 748–756, http://dx.doi.org/10.17531/ein.2020.4.19.

Gearbox faults feature selection and severity classification using machine learning

Indexed by:
Web of Science Group

Ninoslav Zuber [a]*, Rusmir Bajrić [b]

[a] Faculty of Technical Sciences, University of Novi Sad, Trg Dositeja Obradovica 6, 21000 Novi Sad, Serbia
[b] E.ON UK, Westwood Way, Westwood Business Park, Coventry CV4 8LG, United Kingdom

Highlights

- Gearbox health evaluation using vibration features from both time and frequency domains
- Demonstration of importance of data dimension reduction for reliable conclusions.
- Indicators from cepstrum functions had the highest influence in modeling data set.
- Classic impulsiveness indicators had a minor influence in modeling data set.

Abstract

The most widely used technique for gearbox fault diagnosis is still vibration analysis. The need for gearbox condition monitoring in an automated process is essential and there is still a problem with the selection of features that best describe a fault or its severity level. For this purpose, multiple-domain vibration signals statistic features are extracted through time and frequency domain by postprocessing of raw time signal, time-synchronous average signal, frequency spectra and cepstrum. Five different datasets are considered with different levels of fault analyzing gear chipped and a missing tooth, gear root crack, and gear tooth wear under stable running speed and load. A preliminary experimental study of a single stage test bench gearbox was performed in order to test feature sensitivity to type and level of fault in the process of clustering and classification. Selected features were finally processed using an artificial neural network classifier.

Keywords

gearbox fault, vibration analysis, machine learning.

1. Introduction

Condition monitoring systems (CMS) for gearboxes have received considerable attention in the last decade, primarily due to increased number of wind turbines installations and due to the fact that gearbox failure represents a significant part of wind turbines' downtime. CMS helps to ensure the stability, extends the design life of drivetrain element especially gearboxes as a very important part and prevents complete failure, which could be very expensive. Thus, if applied properly, it allows significant savings. In addition to wind turbines, gearboxes are widely known to be used in other industries (energy, mining, petrochemical, automotive, etc.), as an element of high importance responsible for the smooth operation of many productions systems. Also, the availability of the entire system is almost always dependent on the usability of the gearbox.

Gearbox fault can be identified while the defective component is still in operation and repair or replacement can be planned to reduce downtime, increase reliability, maximize availability with the ultimate goal of improving profitability. Gearbox condition monitoring often refers to gearbox diagnostics, which essentially process data with the evaluation of the functionality of a gearbox and detection or identification of faults using condition indicators. Different indicators could be used for gearbox condition monitoring process depending on the interested fault of the type we want to monitor – [3, 4, 13, 15, 25]. Establishing a reliable health detection system, especially for gear fitting faults is the key to ensuring smooth operation of industrial equipment [14].

In literature, fault detection and diagnostics of gears can be obtained by using the time domain analysis. In this case, statistical features, such as Root Mean Square (RMS), Standard Deviation (StD), Kurtosis (KUR), Skewness (SKE), etc., are extracted from vibration signals to perform condition monitoring [16]. On the other hand, the authors in [18] and [30] propose the use of the frequency analysis to identify the characteristic frequencies of the gear defects. Authors in [30] used time synchronous resample (TSR) to pre-process the raw signal to eliminate the interference of asynchronous shaft signal in process of in gearbox fault detection and then the adaptive variational mode decomposition is employed to process the fault synchronous shaft signals obtained by TSR to extract fault features.

Many of these diagnostic methods are based on vibration spectrum analysis or demodulation techniques. The time-domain analysis is primarily performed to track changes during the gear meshing process, while time-domain analysis using the Cepstrum function is used for periodicity monitoring and modulation phenomena in the frequency domain from the sideband components. All of these methods and procedures have found application in the industry and provide relatively reliable diagnostics and often provide gear fault location ability for gearboxes with operation parameters at constant or fairly constant speed and load. However, this approach requires experienced users who will evaluate the status of the gearbox elements by looking at

(*) Corresponding author.
E-mail addresses: N. Zuber - zuber@uns.ac.rs, R. Bajrić - rusmir.bajric@gmail.com

changes in the time or frequency domain relative to the reference condition. The presence of multiple faults usually makes fault identification complex, especially at the early stage of fault when the effects/response are not clear. Hence, introducing a neural network that imitate the ability of human brains to learn from and adapt to the changing environment provides a logical solution – [2, 11]. The techniques such as time-frequency distribution, wavelet transform, statistical feature extraction, multi-scale morphological filters are satisfactorily applied for gear fault identification – [17]. Wang et al. [26] found that the beta kurtosis is a very reliable time-domain diagnostic technique, while phase modulation is sensitive to imperfections in gears. Ibrahim et al. [8] have used the adaptive filtering technique with least mean square algorithm to extract gearbox fault features in this case gear mesh frequency and their sidebands. In [6] authors have proposed a multi-domain manifold method for extracting features from faulty gear and bearing. In [5], using thirteen features from time domain signal and fourteen features from frequency domain, signal have been analysed in study of gear seeded fault detection and the most successful features in time and frequency domain for gear fault identification are extracted and evaluated for compound fault.

Artificial intelligence (AI) based methods tend to replace experienced users and interfere with the gearbox condition assessment process. Generally, they can be divided into supervised learning and unsupervised learning methods. Artificial neural networks (ANN) are the most well-known method of supervised data categorization. The scheme to reduce number of parameters to train neural network in process of intelligent fault diagnosis of gearbox is presented in [15]. How to train a neural network effectively and efficiently is key point. For machine condition monitoring, this has to do in the first place with the choice of parameters to be selected that describe the condition of the machine. Too many features will increase the complexity of the ANN design and at the same increase the training cost and time, and too few features could not provide an accurate representation of the system for the features to ANN rely on [23].

The authors of [10] state that through literature research they have observed that artificial neural networks are the most commonly used classifiers when it comes to intelligent fault diagnosis methods, which consist of two steps: fault feature extraction using signal processing techniques and fault classification using a classifier based on artificial neural networks. The time required to train the neural network as well as the accuracy of the classification is directly related to the number of selected features that are used as input parameters. There may be features that are irrelevant and redundant in the selected feature set. The input feature set can have a large dimensionality that needs to be reduced by excluding irrelevant and redundant features. One of the most popular linear statistical methods often used in the selection of dominant features from a multidimensional data set is the principal component analysis (PCA) – [22], [28]. For example, a PCA-based feature selection scheme was presented to provide guidance on choosing the most representative features from a multi-domain feature set for defect classification in bearing condition monitoring [19]. PCA has been proven efficient dimensionality reduction method for fault diagnosis, effective in the selection of relevant Principal Components (PCs) which describe gearbox state [7].

In this paper, a two-stage feature selection and classification approaches are used. At the first stage, the PCA reduction technique is used and only valuable features are selected for clustering and classification. To approach this challenge, type of fault and the level identification for the most common gear faults (fault modes most frequently occurring in gears), the objective of this paper is to select most valuable features to accurately identify type and also the levels of the selected gear faults. For testing purposes, experimental gearbox test rig with constant speed and load is used with different gear fault types and multiple fault levels with 500 data samples per fault level.

2. Gear fault detection using vibration analysis

Gear vibration content is primarily due to the cyclically variable gear meshing forces. These forces create vibrations that are transmitted to the gearbox housing where they can be measured. The geometry of the gear tooth profile has a crucial influence on the level and pattern of the vibration signals. A perfect sinusoidal gear meshing force would imply the perfect unique tone (single component) of the vibration spectrum, located at the gear mesh frequency. Gear mesh frequency calculated at each stage of the transmission is the product of the number of teeth of the gears and their rotational frequency. With real gears, the surfaces are not ideally smooth and the tooth shape is not ideal, so the vibration spectrum will always contain higher harmonics of the gear mesh frequency combined with other frequency components, like rotational speed and its harmonics (Figure 2). Interaction of frequency components (gear mesh component amplitude variation with rotational speed) in the form of amplitude modulation also indicates the existence of the fault and some processing tools used in gearbox diagnostics are specially developed to identify the sign of modulation in the acquired vibration signal. This can be seen and analysed in time and in frequency domain. Figure 1 shows time synchronous average of the vibration signal from the test bench used in this research (Figure 3). The shape of the signal clearly indicates the amplitude modulation of the higher frequency component (gear mesh frequency) by the lower frequency component (speed of the rotation of the shaft with the faulty gear).

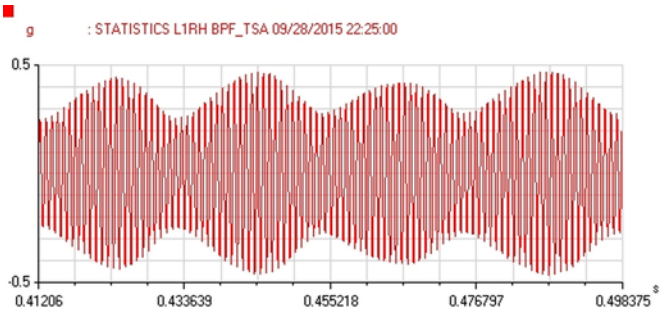

Fig. 1. Time synchronous averaged acceleration signal from the test bench

The existence of amplitude modulation can be seen in the frequency domain too as shown on Figure 2 where regions for the first four harmonics of the gear mesh frequency for the faulty gearbox (Figure 3) are marked. The equidistantly spaced sideband components around each gear mesh component corresponds to the rotational speed of the faulty gear.

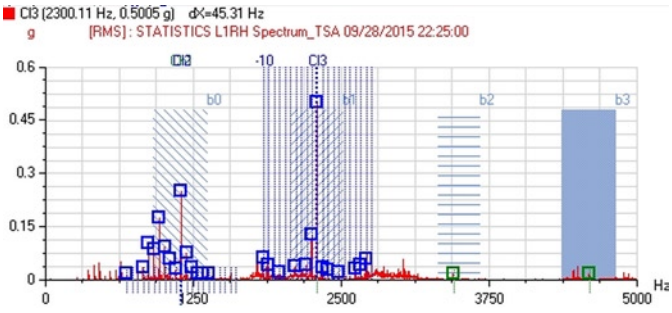

Fig. 2. Frequency spectra of the gearbox with a missing tooth on a gear with marked regions centred around first four harmonics of gear mesh frequency and sideband components

The level of vibrations and content of time waveforms and frequency spectra are also highly influenced by the type and level of the fault (discrete or uniform, early or late stage) and by the load applied to the gearbox. Usability of traditional vibration spectral analysis in reliable detection of faults in the gearbox is limited due to the nature of the signals generated and due to the mentioned influences and character-

istic signal components generated by different faults in gears cannot always be detected using traditional methods [9]. Reliable diagnostics of gearbox health should include advanced methods of signal processing and analysis not just in frequency domain but also in time and time-frequency domains.

The basic procedure for gearbox fault diagnostics is the use of raw time signal spectrum, raw time waveform, and Cepstrum analysis [29]. Unfortunately, such techniques usually work in cases of severe fault presence and when there is not much interference from other high energy components that come from surrounding noise and / or other components. Therefore, it is not aimed for early detection of gearbox fault occurrence and monitoring, which could improve the reliability of the gearbox. Reliable and unambiguous gearbox fault diagnosis becomes a challenge because the interest is primarily in detecting fault at an early stage when it is still minor. Only in that case the end user has time and resources to properly plan its activities in handling the fault by continuous monitoring of its development and planning the best time for production stop in order to perform the required corrective actions defined by the vibration diagnostics and to prevent degradation of gearbox component on time.

When the discrete gear fault is initiated, the vibration signal generated by the fault will have very low amplitudes that will be masked by other components and by the noise and will impossible to detect its presence in the raw signal spectrum. Most proposed methods for diagnosis of gear faults involve noise reduction of recorded signals to facilitate the detection of impulses generated by fault as shown in [1], [20], [21] and [27]. A successful fault detection procedure should, first of all, extract the appropriate frequency content of the measured signal and then detect the presence of a fault in the separated frequency band. Different types of filtering and time synchronous averaging techniques are among the most commonly used techniques for this purpose.

3. Experimental setup

A test bench with a single-stage gearbox was designed and constructed. Several cases were analysed: gear with missing tooth, gear with chipped tooth with two fault levels, crack in the root of the tooth with four fault levels and worn gear pair (surface wear) with three fault levels.

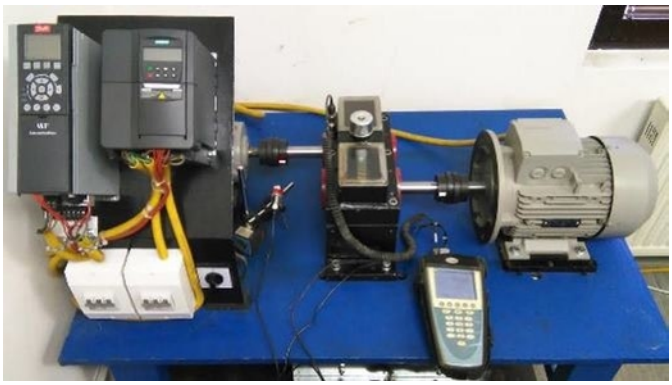

Fig. 3. Gearbox test bench

The test bench used in [3] consists of a single-stage gearbox with an input shaft connected to 2.2 kW AC motor controlled by a frequency inverter (Figure 3). The gearbox output shaft is connected to a 4 kW AC motor controlled by another frequency inverter for load purposes and is used as a DC generator to dissipate the generated energy to the associated resistors. During data collection, gearbox input shaft speed was 46 Hz with 7 Nm of torque (load).

All tests were performed under the same operating conditions, with constant speed and load. The gearbox shafts are aligned with motors to eliminate shaft misalignment influence during the test. An industrial IEPE accelerometer with 100 mV/g sensitivity was used to record the response (vibration) measuring on the bearing housing. An accelerometer is mounted on the bearing housing in a vertical direction using a stud mount. The speed, measured with a contactless laser sensor, and vibration signals are further fed into two-channel vibration data acquisition and analysis system OneproD MVP-2C. The spur gears without profile shift are used with the following characteristics: input gear with 25 teeth, 20 mm wide and output gear with 57 teeth, 21 mm wide, 3.0 mm modules with a pressure angle of 10.26 degrees.

Different levels of the simulated fault of the chipped gear are shown in Figure 4. The fault was introduced using a milling tool with 40 mm diameter. The size of this fault in two steps ranged from 0.25 and 0.5 to the gear width, while for the missing tooth fault this width corresponded to the complete width of the gear, marked as “c”on Figure 4. These cases were labelled as OZ0 for healthy gear, OZ1 for 0.25c, OZ2 for 0.5c fault and OZ3 for gear with one missing tooth.

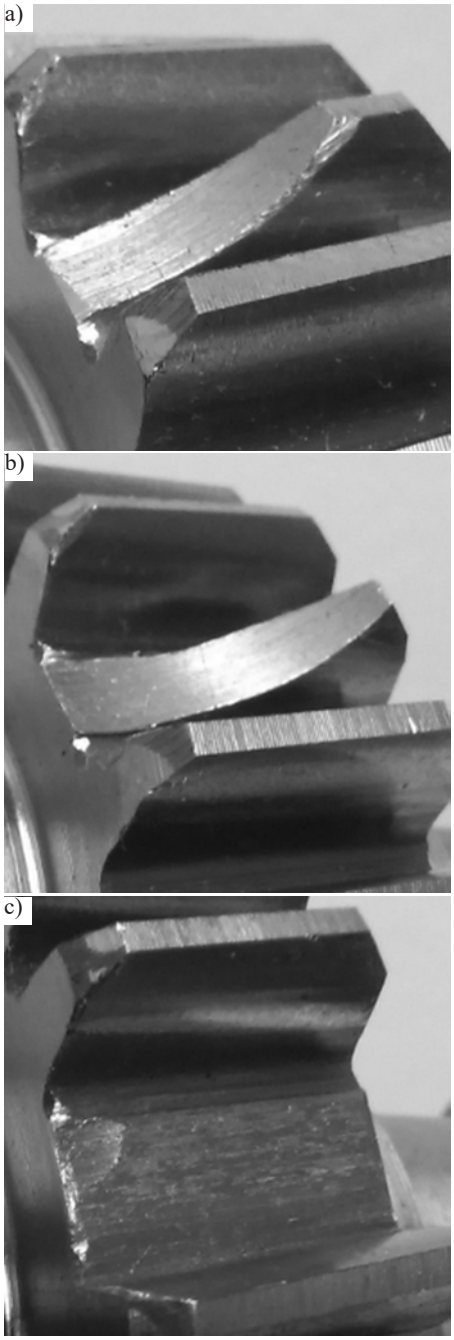

Fig. 4. Different gear tooth chipped levels (a) – 0,25c; (b) – 0.50c; (c) c – 1c

Also, investigation in case of simulated gear crack was carried out. The cracks at the root of the tooth were introduced using an electrical

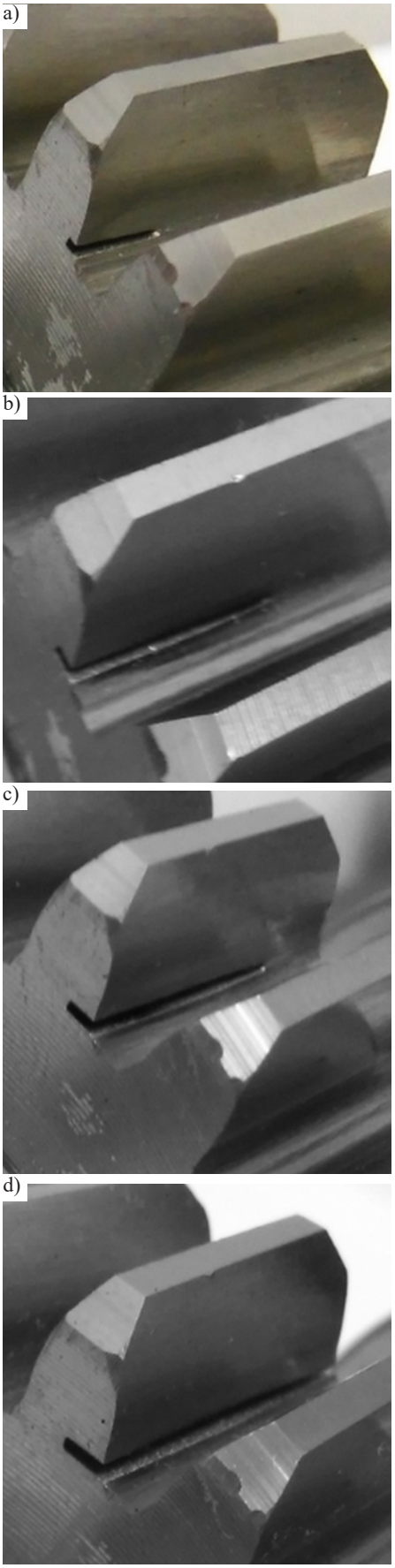

Fig. 5. The four different gear crack levels: (a) crack level 25%; (b) crack level 50%; (c) crack level 75%; (d) crack level 100%

discharge machine with an electrode 0.5mm thick. For the simulation of the different gear crack levels, the crack depths were 0.25, 0.5, 0.75 and 1 times the half of the chordal tooth thickness, respectively, because the tooth will break rapidly when the crack depth is more than half of the chordal tooth thickness [24]. Here, the chordal tooth thickness was d = 4.78 mm at the pitch line. The crack widths were 0.25, 0.5, 0.75, and one times the face width c = 20 mm, respectively, as shown on Figure 5. The width of the gear crack through five steps ranged 0 (label PRS0), 0.25 (label PRS5), 0.5 (label PRS10),

Table 1. Dimension of cracks for different crack levels

Crack dimension [%]	Depth [mm]	Width [mm]	Height [mm]
25% (label PRS5)	0.5975 mm	5 mm	0.5 mm
50% (label PRS10)	1.195 mm	10 mm	0.5 mm
75% (label PRS15)	1.7925 mm	15 mm	0.5 mm
100% (label PRS20)	2.39 mm	20 mm	0.5 mm

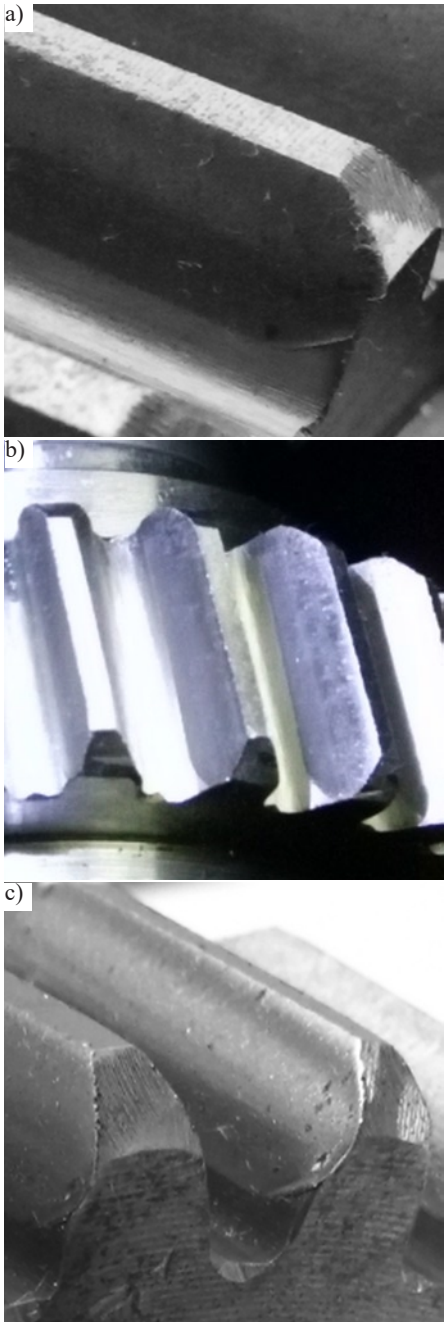

Fig. 6. The three different gear wear levels: (a) wear level H1; (b) wear level H2; (c) wear level H3

0.75 (label PRS15), and 1 (label PRS20) times the face width c of the gear. Dimensions of different gear cracks are shown in Table 1.

Different gear wear faults (in three steps) are introduced in such a way that a certain amount of quartz sand was inserted into the lubricating oil and the gearbox operated for 10 minutes under the same operation condition. After each step measure over the pins was performed to determine tooth thickness. In this case, gear tooth wear level was measured for driving and driven gear. The number of teeth used during measurement over the pins was four for driving gear and seven for the driven gear, all in accordance with [31]. A micrometer screw gage with 0.001mm accuracy was used during measurement over the pins. The final measurements over the teeth on both gears were determined by the arithmetic mean of 8 measurements at different positions along with the scope of the gears. The wear of the driving gear was calculated as the difference of this measurement to the measurement from the undamaged gear and these 3 levels of difference, in this case levels of gear wear, were: 0.094 mm (label H1), 0.311 mm (Label H2) and 0.433mm (Label H3), as shown on Figure 6.

4. Methodology, procedure and detection results

Fault diagnosis methods are mainly based on fault features extracted by some signal processing techniques. In this paper the authors of this research tested all cases of introduced gear faults and optimal set of the features with the highest percentage of classification selected. The methodology consists of the following steps:

1. Extraction of 32 features (according to Figure 7 and Table 2) from time and frequency domains in order to determine/verify the potential for diagnostics of different gear faults.
2. Clustering selected number of features through Kohonen's self-organized maps [12] and quality evaluation of feature clustering through quantization error.
3. Classification of selected number of features and assessment of the percentage classification success considering the overall set of features.
4. Application of PCA and selection of the most influential features.
5. Classification of selected number of features after PCA, with an assessment of the classification success rate considering the reduced feature set.
6. Finally, the features with the highest percentage of classification were selected and their potential in identifying gear faults that are more useful in the classification process and more accurate type and level of gear fault assessment using ML were identified.

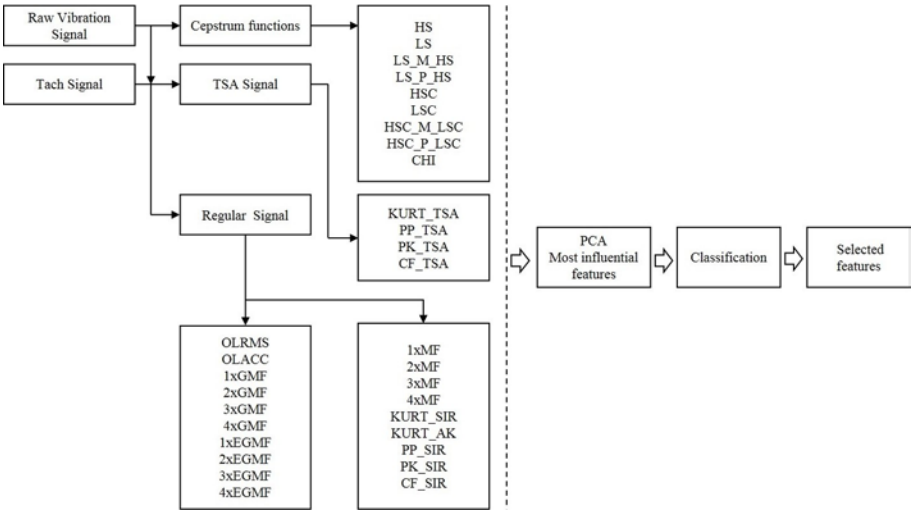

Fig. 7. Proposed methodology processing flow for feature selection

Figure 7 illustrates the workflow of proposed methodology for analysed gear fault types.

Amplitudes of the GM components were extracted from the acquired frequency spectra. Energies around each GM component are actually RMS of amplitudes inside discrete frequency bands centred around each GM components and ±5X wide where X stands for the rotational speed of the input shaft. This way five modulation sidebands are included from each side of the GM component, as a central frequency. Modulation factor is a ratio of GMF and EGMF at each harmonic of GMF. Kurtosis as the fourth standardized moment of the time signal was used since its sensitivity to impact components in the signal and one of the most traditional and probably also the most widely employed feature [1]. Kurtosis from raw signal, from time synchronous average and from autocorrelation of the raw signal were used. Extractions from cepstrum functions and their different combinations (sum, difference, ratio) were used in order to evaluate the full potential of cepstrum function in gearbox diagnostics. Crest factor is the ratio of peak and RMS value and the crest factor from raw and synchronous time average were used. For each induced gear fault total of 500 independent recordings were acquired.

5. Diagnostic and detection results

The above-mentioned methodology has been applied to all analysed faults separately (chipped tooth, missing tooth, cracked tooth, gear wear). In this paper, the results of diagnostics and detection of faults will be demonstrated on a complete data set which consists of all the data for all analysed cases i.e. for all 12 fault cases (labels). In order to develop self-organized Kohonen maps (SOM), Matlab programming environment and SOM Toolbox version 2.0 were used – [32].

First, detection of the type and level of gear fault was performed using an input matrix with 32 extracted vibration features – this was a complete set of input features. The quantization error (qe) is calculated as the mean distance between the input vectors and their winning neurons and is used as an estimate of the map resolution. As a method of normalization of input vectors in all Kohonen maps covered in this paper, the "var" method was used in which all input features after normalization have variance of 1.

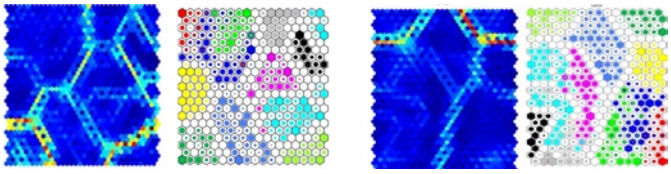

Fig. 8. Distance matrix and SOM topology with color coded labels for complete set of 32 features (left) and for the reduced set of 16 features (right)

The result of the training of SOM when using the complete set of input features is a map with a quantization error of 1.656 (Figure 8 - left). As noted, in order to develop a model for identifying the gear state or classifying, both, the fault type and its level, multilayer perceptron neural networks (MLP) using supervised training methods, with the propagation of the output error backward and with a single layer of hidden neurons were used. The number of input neurons is defined by the dimensionality of the input vector, while the number of output neurons is defined by the type of problem. Each case covered by the experimental part of this paper was solved using neural networks analysed with 30 different neural network configurations. The following network parameters were varied: number of neurons in the hidden layer and type

Table 2. Extracted vibration features

Parameter	Label	Parameter	Label
RMS of vibration velocity [mm/s] in range 10 Hz–1 kHz	OLRMS	Kurtosis from raw signal postprocess with autocorrelation	KURT_AK
RMS of acceleration [g] in range 10 Hz–20 kHz	OLACC	Amplitude of driving gear rahmonic peak	HS
Amplitude of gear mesh (GM) frequency	1xGMF	Amplitude of driven gear rahmonic peak	LS
Amplitude of GM 2nd harmonic	2xGMF	Difference of driven and driving gear rahmonic peak	LS_M_HS
Amplitude of GM 3rd harmonic	3xGMF	Sum of driven and driving gear rahmonic peak	LS_P_HS
Amplitude of GM 4th harmonic	4xGMF	Ratio of driving gear rahmonic peak and undamaged (new) driving gear rahmonic peak	HSC
Energy around GM frequency	1xEGMF	Ratio of driven gear rahmonic peak and undamaged (new) driven gear rahmonic peak	LSC
Energy around GM frequency 2nd harmonic	2xEGMF	Difference between HSC and LSC	HSC_M_LSC
Energy around GM frequency 3rd harmonic	3xEGMF	Sum of HSC and LSC	HSC_P_LSC
Energy around GM frequency 4th harmonic	4xEGMF	Cepstrum Health Indicator – ratio of „HSC_M_LSC“ and „HSC_P_LSC“	CHI
Modulation factor around GM	1xMF	Peak-to-peak amplitude from raw signal	PP_SIR
Modulation factor around GM 2nd harmonic	2xMF	Peak-to-peak amplitude from time synchronous average	PP_TSA
Modulation factor around GM 3rd harmonic	3xMF	Peak amplitude from raw signal	PK_SIR
Modulation factor around GM 4th harmonic	4xMF	Peak amplitude from time synchronous average	PK_TSA
Kurtosis from raw signal	KURT_SIR	Crest factor (CF) from raw signal	CF_SIR
Kurtosis from time synchronous averaged signal	KURT_TSA	Crest factor (CF) from time synchronous averaged signal	CF_TSA

Table 3. Confusion matrix for the best MLP trained with a complete set of 32 input feature.

Label:	H1	H2	H3	OZ0	OZ1	OZ2	OZ3	PRS0	PRS10	PRS15	PRS20	PRS5	All
Total	500	500	500	500	500	500	500	500	500	500	501	500	6001
Correct %	80.8	96.2	89	86.6	77	66	81.6	99.8	90.2	94.6	97.4052	99	**88.185**
Incorrect %	19.2	3.8	11	13.4	23	34	18.4	0.2	9.8	5.4	2.5948	1	11.815

Table 4. Eigenvectors individual and cumulative variance for PCs

	Eigenvalues	% Total variance	Cumulative %
PC1	8.701992	27.19373	27.19373
PC2	7.603384	23.76058	50.9543
PC3	3.788634	11.83948	62.79378
PC4	3.054879	9.5465	72.34028
PC5	2.424033	7.5751	79.91538
PC6	1.202408	3.75753	83.67291
PC7	0.870788	2.72121	86.39412

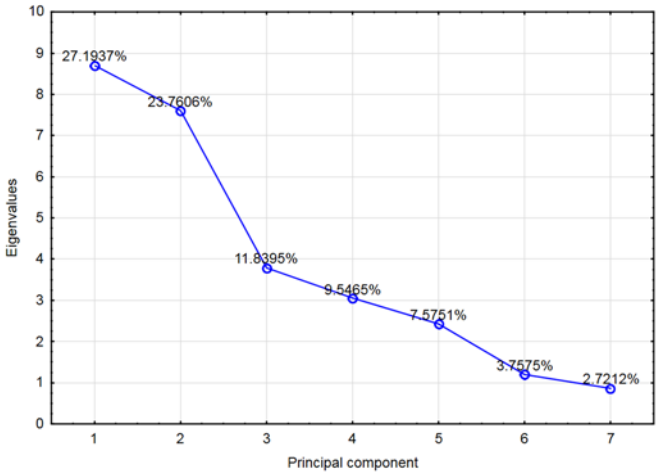

Fig. 9. Scree plot

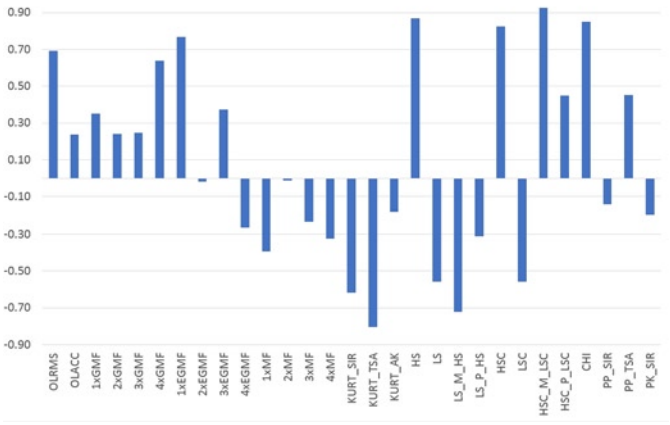

Fig. 10. Loadings for PC1

of activation functions of the neurons in the hidden layer. At the end of testing different network configurations, only one configuration with the best prediction results was selected as a winner. In case of using the complete set of 32 input features, the confusion matrix of the network is presented in Table 3. This network had 17 neurons in the hidden layer and had a prediction success of 88.19%.

PCs with eigenvalues above 1 are the first six PCs and, according to Kaiser's criterion, we can choose them so that in the reduced dimension we describe the original input dataset with 83.67% of the variance (Figure 9).

In order to find a prediction algorithm with better performance, a PCA is performed on the complete input dataset with 32 features to define a new a dataset with a reduced dimension. As a result of PCA, 7 principal components (PCs) have been extracted with the eigenvalues shown on Table 4. For this new space of variables, the most influential variables are the variables with the highest loadings which are pro-

Table 5. Modeling power for each feature and its importance to PC model

Feature	Power	Importance		Feature	Power	Importance
LS_M_HS	0.991223	1		KURT_SIR	0.896093	17
LS	0.990368	2		2xEGMF	0.893102	18
LS_P_HS	0.988442	3		3xGMF	0.873908	19
HS	0.987037	4		CF_TSA	0.83275	20
HSC	0.979869	5		3xMF	0.813719	21
HSC_M_LSC	0.979868	6		1xMF	0.813074	22
HSC_P_LSC	0.967299	7		PP_TSA	0.79878	23
LSC	0.960409	8		2xMF	0.785357	24
OLACC	0.946683	9		CF_SIR	0.772903	25
CHI	0.923562	10		KURT_TSA	0.769628	26
3xEGMF	0.923215	11		4xEGMF	0.759167	27
PP_SIR	0.921343	12		PK_TSA	0.756958	28
2xGMF	0.920716	13		1xGMF	0.749699	29
1xEGMF	0.916267	14		4xGMF	0.741551	30
PK_SIR	0.910155	15		4xMF	0.709164	31
OLRMS	0.909475	16		KURT_AK	0.464335	32

Table 6. Confusion matrix for the best MLP trained with a reduced set of 16 input features

Label:	H1	H2	H3	OZ0	OZ1	OZ2	OZ3	PRS0	PRS10	PRS15	PRS20	PRS5	All
Total	500	500	500	500	500	500	500	500	500	500	501	500	6001
Correct %	100	100	100	99.2	97.8	97.6	99.8	100	100	91	98.6028	100	98.667
Incorrect %	0	0	0	0.8	2.2	2.4	0.2	0	0	9	1.3972	0	1.333

jections on these dominant PCs. Loadings for each variable for first principal component (PC1) are shown on Figure 10.

The importance of each feature is calculated through a modelling power – features with the highest modelling power are the most relevant for the PC model. Table 5 shows modelling power for each of the 32 input features and its importance. As relevant features, the first 16 were chosen and this defined the reduced set of input features.

With this new – reduced set of input features MLP ANN training is performed and the new best configuration is obtained – a network with 16 hidden neurons and with a much better prediction success 98.67%, compared to 88.19% in the case of using a complete set of input features. Confusion matrix for this network is shown in Table 6.

6. Conclusion

Identification of the health condition of complex rotating machines like gearboxes where a highly skilled and experienced vibration analyst is needed to set up the vibration measurement and to evaluate the results is much easier using automatic fault diagnostics methods, such as supervised and unsupervised ANN. To build an accurate and reliable ANN an optimal set of vibration input features is needed. An optimal set of input features defines not just a good definition of scalar parameters obtained from the time and frequency domains but also the total number of the features. The authors of this research tested all cases of introduced gear faults and optimal sets were defined for each case. In this paper a part of the research is presented – the case where all introduced gear faults were analysed. For this universal case, an optimal set of input vibration features is proposed and its selection is verified through the increase of ANN prediction accuracy. Use of all 32 input features resulted in acceptable 88.19% prediction accuracy. Dimension reduction, as expected, resulted in better prediction accuracy of 98.67%. This was especially true for cases of chipped gear where the percentage of incorrect guess from 34% in case of label OZ2 for example, came down to 2.4%. These results correspond to cases where speed and load are constant. This set of input features can be used not just for ANN modelling but also for manual monitoring of gearbox health. In addition to this, it is worth to mention that the first eight dominant features are from the cepstrum function which is, although well known for long time, most of the time unused in many commercial systems for rotating machines vibration condition monitoring. This could motivate vibration analysts to use extractions from the cepstrum function as a regular part of their vibration data collection routes. Content of the cepstrum function is related to modulation phenomena in signals. Overall acceleration together with the kurtosis parameter and crest factor are indicators of impulsiveness inside a signal that is expected in case of discrete faults on gears. Crest factors and kurtosis parameters on different time signals had a minor modelling power.

References

1. Antoni J, Borghesani P. A statistical methodology for the design of condition indicators. Mechanical Systems and Signal Processing 2019; 114: 290-237, https://doi.org/10.1016/j.ymssp.2018.05.012.
2. Baillie D, Mathew J. A comparison of autoregressive modeling techniques for fault diagnosis of rolling element bearings. Mechanical Systems and Signal Processing 1996; 10: 1-17, https://doi.org/10.1006/mssp.1996.0001.
3. Bajrić R. Contribution to the identification of gear pairs damage by using mechanical vibration signal analysis techniques. PhD Thesis, Faculty of Technical Sciences -University of Novi Sad 2016
4. Chen Y, Liang X, Zuo MJ. Sparse time series modeling of the baseline vibration from a gearbox under time-varying speed condition. Mechanical Systems and Signal Processing 2019; 134: 106342, https://doi.org/10.1016/j.ymssp.2019.106342.
5. Dhamande LS, Chaudhari MB. Compound gear-bearing fault feature extraction using statistical features based on time-frequency method. Measurement 2018; 125: 63-77, https://doi.org/10.1016/j.measurement.2018.04.059.
6. Gan M, Wang C, Zhu C. Multiple-domain manifold for feature extraction in machinery fault diagnosis Measurement 2015; 75: 76-91, https://doi.org/10.1016/j.measurement.2015.07.042.
7. He Q, Yan R, Fanrang K, Du R. Machine condition monitoring using principal component representations. Mechanical Systems and Signal Processing 2009; 23(2): 446-466, https://doi.org/10.1016/j.ymssp.2008.03.010.
8. Ibrahim G, Albarbar A, Abouhnik A, Shnibha R. Adaptive filtering based system for extracting gearbox condition feature from the measured vibrations. Measurement 2013; 46 (6): 2029-2034, https://doi.org/10.1016/j.measurement.2013.02.019.
9. Jardine AK, Lin D, Banjevic D. A review on machinery diagnostics and prognostics implementing condition-based maintenance. Mechanical Systems and Signal Processing 2006; 20(7): 1483-1510, https://doi.org/10.1016/j.ymssp.2005.09.012.
10. Jia F, Lei Y, Lin J, Zhou X, Lu N. Deep neural networks: A promising tool for fault characteristic mining and intelligent diagnosis of rotating machinery with massive data. Mechanical Systems and Signal Processing 2016, 72: 303-315, https://doi.org/10.1016/j.ymssp.2015.10.025.
11. Karabacak YE, Gursel Özmen N, Gumusel L. Worm gear condition monitoring and fault detection from thermal images via deep learning method. Eksploatacja i Niezawodnosc - Maintenance and Reliability 2020; 22 (3): 544-556, https://doi.org/10.17531/ein.2020.3.18.
12. Kohonen T. Self-Organizing Maps. Berlin: Springer, 1995, https://doi.org/10.1007/978-3-642-97610-0.
13. Lazarz B, Wojnar G, Czech P. Early fault detection of toothed gear in exploitation conditions. Eksploatacja i Niezawodnosc - Maintenance and Reliability 2011; 1(49): 68-77
14. Li X, Li J, He D, Qu Y. Gear pitting fault diagnosis using raw acoustic emission signal based on deep learning. Eksploatacja i Niezawodnosc - Maintenance and Reliability 2019; 21 (3): 403-410, https://doi.org/10.17531/ein.2019.3.6.
15. Li Y, Wang K. Modified convolutional neural network with global average pooling for intelligent fault diagnosis of industrial gearbox. Eksploatacja i niezawodnosc - Maintenance and Reliability 2020; 22 (1): 63-72, https://doi.org/10.17531/ein.2020.1.8.
16. Liu S, Hou S, He K, Yang W. L-kurtosis and its application for fault detection of rolling element bearings, Measurement 2018, 116: 523-532, https://doi.org/10.1016/j.measurement.2017.11.049.
17. Loutas TH, Roulias D, Pauly E, Kostopoulos V. The combined use of vibration, acoustic emission and oil debris on-line monitoring towards a more effective condition monitoring of rotating machinery. Mechanical Systems and Signal Processing 2011; 25 (4): 1339-1352, https://doi.org/10.1016/j.ymssp.2010.11.007.
18. Lu D, Qiao W, Gong X. Current-based gear fault detection for wind turbine gearboxes, IEEE Transactions on Sustainable Energy 2017, 8 (4): 1453-1462, https://doi.org/10.1109/TSTE.2017.2690835.
19. Malhi A, Gao R X. PCA-based feature selection scheme for machine defect classification. IEEE Transactions on Instrumentation and Measurement 2004, 53 (6): 1517 - 1525, https://doi.org/10.1109/TIM.2004.834070.
20. Omar FK, Gaouda A. Dynamic wavelet-based tool for gearbox diagnosis. Mechanical Systems and Signal Processing 2012; 26(1): 190-204, https://doi.org/10.1016/j.ymssp.2011.06.021.

21. Rafiee J, Rafiee M, Tse P. Application of mother wavelet functions for automatic gear and bearing fault diagnosis. Expert Systems with Applications 2010, 37: 4568-4579, https://doi.org/10.1016/j.eswa.2009.12.051.
22. Schweizer K, Cattin PC, Brunner R, Müller B, Huber C, Romkes J. Automatic selection of a representative trial from multiple measurements using Principle Component Analysis, Journal of biomechanics 2012; 45: 2306-2309, https://doi.org/10.1016/j.jbiomech.2012.06.012.
23. Stetco A, Dinmohammadi F, Zhao X, Robu V, Flynn D, Barnes Keane MJ, Nenadic G. Machine learning methods for wind turbine condition monitoring: A review. Renewable Energy 2019; 133: 620-635, https://doi.org/10.1016/j.renene.2018.10.047.
24. Wang D. K-nearest neighbors based methods for identification of different gear crack levels under different motor speeds and loads: Revisited. Mechanical Systems and Signal Processing 2016; 70-71: 201-208, https://doi.org/10.1016/j.ymssp.2015.10.007.
25. Wang L, Shao Y. Fault feature extraction of rotating machinery using a reweighted complete ensemble empirical mode decomposition with adaptive noise and demodulation analysis. Mechanical Systems and Signal Processing 2020; 138: 106545, https://doi.org/10.1016/j.ymssp.2019.106545.
26. Wang W.Q., Ismail F., Golnaraghi M. Assessment of gear damage monitoring techniques using vibration measurements. Mechanical Systems and Signal Processing 2001; 15 (5): 905-922, https://doi.org/10.1006/mssp.2001.1392.
27. YanPing Z, ShuHong H, JingHong H, Tao S, Wei L. Continuous wavelet grey moment approach for vibration analysis of rotating machinery, Mechanical Systems and Signal Processing 2006; 20(5): 1202-1220, https://doi.org/10.1016/j.ymssp.2005.04.009.
28. Widodo A, Yang BS, Han T. Combination of independent component analysis and support vector machines for intelligent faults diagnosis of induction motors. Expert Systems with Applications 2007; 32(2): 299-312, https://doi.org/10.1016/j.eswa.2005.11.031.
29. Ziaran S, Darula R. Determination of the state of wear of high contact ratio gear sets by means of spectrum and cepstrum analysis. Journal of Vibration and Acoustics 2013; 135(2): 021008, https://doi.org/10.1115/1.4023208.
30. Zhang X, Zhao J. Compound fault detection in gearbox based on time synchronous resample and adaptive variational mode decomposition. Eksploatacja i Niezawodnosc - Maintenance and Reliability 2020; 22 (1): 161-169, https://doi.org/10.17531/ein.2020.1.19.
31. ISO 21771: 2007 Gears - Cylindrical involute gears and gear pairs - Concepts and geometry
32. SOM Toolbox for Matlab, laboratory for information and computer science, University of Helsinki, http://www.cis.hut.fi/projects/somtoolbox